Synthesis and structural and theoretical characterization of a nickel(0) complex of tribenzocyclyne (TBC) and the preparation of a novel organometallic conductor

Joseph D. Ferrara, Auro A. Tanaka, Cristian. Fierro, Claire A. Tessier-Youngs, and Wiley J. Youngs

Organometallics, **1989**, 8 (9), 2089-2098• DOI: 10.1021/om00111a001 • Publication Date (Web): 01 May 2002

Organometallics is published by the American Chemical Society. 1155 Sixteenth Street N.W., Washington, DC 20036

ORGANOMETALLICS

Volume 8, Number 9, September 1989

Synthesis and Structural and Theoretical Characterization of a Nickel(0) Complex of Tribenzocyclyne (TBC) and the Preparation of a Novel Organometallic Conductor

Joseph D. Ferrara, Auro A. Tanaka, Cristian Fierro, Claire A. Tessier-Youngs, and Wiley J. Youngs*

Department of Chemistry, Case Western Reserve University, Cleveland, Ohio 44106-2699

Received July 25, 1988

Reaction of $Ni(COD)_2$ with TBC in benzene affords a planar nickel(0) complex, Ni(TBC), with the nickel atom coordinated equally by all three alkynes of the TBC ligand. The complex crystallizes in the noncentrosymmetric space group $Pna2_1$ with a = 15.518 (3) Å, b = 18.761 (4) Å, c = 5.375 (1) Å, V = 1564.8 (5) Å^3, and Z = 4. The nickel–carbon and carbon–carbon (alkyne) bond lengths average 1.958 (5) and 1.240 (10) Å, respectively. The molecules are slipped-stacked in an eclipsed conformation with an interplanar spacing of 3.35 (1) Å. The reaction chemistry of Ni(TBC) with several small molecules including H_2O, $CDCl_3$, CO, CO_2, O_2, and CH_3CN has been explored. The rates of reaction with CO and O_2 are solvent-dependent. Electrochemical studies of Ni(TBC) and TBC show two reduction waves which are moderately reversible. ASED-MO calculations on Ni(TBC) indicate the HOMO is primarily metal centered, whereas the LUMO is ligand centered. Ni(TBC) is reduced with lithium, sodium, and potassium in various solvents (THF and DME) in the presence of various chelating agents (TMEDA, 18-crown-6, and cryptand-(2.2.2)) to the monoanion and dianion. The material $[K(C222)]_2[Ni(TBC)]$ was combined with Ni(TBC) to yield a conducting material. The maximum conductivity (via two-probe powder compaction) was observed to be 2×10^{-3} $(\Omega\ cm)^{-1}$ at 0.5 electron per Ni(TBC) unit. A parallel study on TBC showed a maximum conductivity of 8 (2) $\times 10^{-5}$ $(\Omega\ cm)^{-1}$ at 0.6 electron per TBC unit.

Introduction

Transition-metal complexes of planar metallomacrocycles, including ligand systems such as the porphyrins[1] and phthalocyanines,[2] have been studied in depth as precursors for one-dimensional conductors. These complexes have several key features in common: the molecules are planar with an extended π-system, the ligand atoms which complex the metal are relatively hard nitrogen donors, the ligand has a formal negative oxidation state, and the complexes can be made conductors by either oxidation[2] or reduction.[3] The possibility of using a softer, more polarizable donor is realized with cyclyne ligands, macrocyclic polyalkynes,[4-9] which have available carbon–carbon

---

(1) (a) Hoffman, B. M.; Ibers, J. A. *Acc. Chem. Res.* **1983**, *16*, 15–21. (b) Phillips, T. E.; Scaringe, R. P.; Hoffman, B. M.; Ibers, J. A. *J. Am. Chem. Soc.* **1980**, *102*, 3435–3443. (c) Ferraro, J. R.; Williams, J. M. *Introduction to Synthetic Electrical Conductors*; Academic Press: New York, 1987.

(2) (a) Ibers, J. A.; Page, C. J.; Martinsen, J.; Hoffman, B. M. *Struct. Bonding (Berlin)* **1982**, *50*, 1–55. (b) Marks, T. J. *Science (Washington, DC)* **1985**, *227*, 881–889. (c) Diel, B. N.; Inabe, T.; Jaggi, N. K.; Lyding, J. W.; Schneider, O.; Hannack, M.; Kannewurf, C. R.; Marks T. J.; Schwartz, L. H. *J. Am. Chem. Soc.* **1984**, *106*, 3207–3214. (d) Diel, B. N.; Inabe, T.; Lyding, J. W.; Schock, K. F.; Kannewurf, C. R.; Marks, T. J. *J. Am. Chem. Soc.* **1983**, *105*, 1551–1567. (e) Schramm, C. S.; Scaringe, R. P.; Stojakovic, D. R.; Hoffman, B. M.; Ibers, J. A.; Marks, T. J. *J. Am. Chem. Soc.* **1980**, *102*, 6702–6713. (f) Petersen, J. L.; Schramm, C. S.; Stojakovic, D. R.; Hoffman, B. M.; Marks, T. J. *J. Am. Chem. Soc.* **1977**, *99*, 286–288. (g) Martinsen, J.; Stanton, J. L.; Greene, R. L.; Tanaka, J.; Hoffman, B. M.; Ibers, J. A. *J. Am. Chem. Soc.* **1985**, *107*, 6915–6920.

(3) (a) Dirk, C. W.; Mintz, E. A.; Schoch, K. F.; Marks, T. J. *J. Macromol. Sci., Chem.* **1981**, *A16*, 275–298. (b) Le Moigne, J.; Even, R. *J. Chem. Phys.* **1985**, *83*, 6472–6479.

(4) (a) Staab, H. A.; Graf, F. *Chem. Ber.* **1970**, *103*, 1107–1118. (b) Staab, H. A.; Graf, F. *Tetrahedron Lett.* **1966**, 751–757. (c) Campbell, I. D.; Eglington, G.; Henderson, W.; Raphael, R. A. *J. Chem. Soc., Chem. Commun.* **1966**, 87–89.

(5) Nakagawa, M. In *The Chemistry of the Carbon–Carbon Triple Bond*, Part 2 Patai, S., Ed.; Wiley: Chichester, 1978; pp 635–712.

(6) (a) Sondheimer, F. *Acc. Chem. Res.* **1972**, *5*, 81–91. (b) Sondheimer, F. *Proc. R. Soc. London, Ser. A* **1967**, *297*, 173–204. (c) Sondheimer, F. *Pure Appl. Chem.* **1963**, *7*, 363–388. (d) Akiyama, S.; Nakagawa, M. *Chem. Ind. (London)* **1960**, 346–7. (e) Akiyama, S.; Nakagawa, M. *Bull. Chem. Soc. Jpn* **1960**, *33*, 1293–1298. (f) Akiyama, S.; Misumi, S.; Nakagawa, M. *Bull. Chem. Soc. Jpn.* **1962**, *35*, 1829–1836. (g) Okamura, W. H.; Sondheimer, F. *J. Am. Chem. Soc.* **1967**, *89*, 5991–2. (h) Behr, O. M.; Eglington, G.; Lardy, I. A.; Raphael, R. A. *J. Chem. Soc.* **1964**, 1151–61. (i) Wolovsky, R.; Sondheimer, F. *J. Am. Chem. Soc.* **1965**, *87*, 5720–27. (j) Behr, O. M.; Eglington, G.; Galbraith, A. R.; Raphael, R. A. *J. Chem. Soc.* **1960**, 3614–3625. (k) Staab, H. A.; Mack, H.; Wehinger, E. *Tetrahedron Lett.* **1966**, 1465–69. (l) Staab, H. A.; Neunhoeffer, K. *Synthesis* **1974**, 424. (m) Untch, K. G.; Wysocki, D. C. *J. Am. Chem. Soc.* **1966**, *88*, 2608–10.

0276-7333/89/2308-2089$01.50/0

triple bonds for coordination to metal atoms or ions. The cyclyne TBC,[4] which has a 12-membered antiaromatic ring system, is shown below.

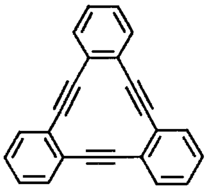

TBC

An important feature of this compound is that the distance from the centroid of the 12-membered ring to the centroid of the C≡C bonds is approximately 2.1 Å. This distance is typical of π-alkyne transition-metal bonding interactions.[10,11] The crystal structure shows TBC[12] to be nearly planar.

The π-coordination of three alkene ligands to give complexes NiL_3 has been previously observed. Early interest in such complexes was related to work on Ziegler–Natta catalysts and the nickel(0)-catalyzed cyclotrimerization of dienes.[13] The crystal structure of Ni(*E*,*E*,*E*-CDT)[14] (CDT = 1,5,9-cyclododecatriene) shows the alkenes in a trigonal arrangement around the Ni(0) center with the alkene groups twisted slightly out of the plane, whereas the crystal structure of tris(norbornene)nickel(0)[15] shows that the alkenes are in a trigonal plane about the nickel center. This is consistent with theoretical calculations which show the preferred orientation for three alkenes coordinated to Ni(0) is a trigonal plane with the carbon–carbon double bonds in the plane.[16] Previous to our preliminary report,[17a] alkynes had not been observed to form NiL_3 complexes. For example, reaction of $Ni(COD)_2$ with diphenylacetylene has been shown to yield $Ni_2(PhC{\equiv}CPh)(COD)_2$.[18] The present work shows that the reaction of $Ni(COD)_2$ with TBC in benzene affords a Ni(0) complex in which the nickel atom resides in the cavity of the 12-membered ring equally bound to all three alkynes. The synthesis, characterization, and reaction chemistry of Ni(TBC) is presented below. In addition, the preparation of n-doped macrocyclic conductors based upon TBC and Ni(TBC) is reported.[17b]

Experimental Section

General Data. All manipulations were performed under argon or vacuum by using standard inert-atmosphere techniques[19] unless specified otherwise. Solvents were distilled from sodium/benzophenone ketyl unless specified otherwise. Tetramethylethylenediamine (TMEDA) was purified by vacuum distillation from BaO. The crown ether 18-crown-6 was purified by sublimation from sodium/benzophenone ketyl. Cryptand-(2.2.2) (C222, Kryptofix-222, Aldrich) was used as received and stored in a drybox. The alkali metals used were lithium sand (Aldrich, 1% sodium), sodium powder (Aldrich), and potassium ingot (Aldrich gold label). The $Ni(COD)_2$ (Aldrich, Strem) was vacuum sublimed at 110 °C and 10^{-4} Torr and used within 24 h. Tetra-*n*-butylammonium perchlorate (TBAP, Fisher, polarographic grade) and $LiBF_4$ (Alfa) were dried at 50 °C at 10^{-3} Torr for 16 h. Lithium foil (Foote, H. P.) was scraped clean prior to each use. Carbon monoxide (Matheson, anhydrous) was passed through a -196 °C trap to remove impurities. Infrared spectra were recorded on a Mattson Cygnus 25 FT-IR. Nuclear magnetic resonance spectra were recorded on either a Varian XL-200 or a Bruker MSL-400 FT-NMR spectrometer.[20] Ultraviolet-visible spectra were recorded on a Cary 14 or a Varian 2300 spectrophotometer. Electron paramagnetic resonance spectra were recorded on a Varian E-12 spectrometer equipped with a Nicolet signal averager and referenced externally with diphenylpicrylhydrazyl (DPPH). Elemental analysis was performed by Schwarzkopf Microanalytical Laboratories.

Synthesis of TBC. TBC was prepared via the Stephens–Castro coupling[21] of copper(I) *o*-iodophenylacetylide.[4c] The *o*-iodophenylacetylene was synthesized from phenylacetylene by modification of a literature procedure.[22] The complete FT-IR and FT-NMR are reported here. IR (Nujol): 3059 w, 2217 vk (C≡C), 1961 vw, 1951 vw, 1940 vw, 1927 vw, 1896 vw, 1849 vw, 1817 vw, 1737 vw, 1620 w, 1588 w, 1487 s, 1286 w, 1272 w, 1259 w, 1163 w, 1157 w, 1154 w, 1088 w, 1038 w, 951 w, 833 w, 755 vs,

---

(7) (a) Scott, L. T.; DeCicco, G. J.; Hyun, J. L.; Reinhardt, G. *J. Am. Chem. Soc.* **1985**, *107*, 6546–6555. (b) Houk, K. N.; Scott, L. T.; Rondan, N. G.; Spellmeyer, D. C.; Reinhardt, G.; Hyun, J. L.; DeCicco, G. J.; Weiss, R.; Chen, M. H. M.; Bass, L. S.; Clardy, J.; Jorgensen, F. S.; Eaton, T. A.; Sarkozi, V.; Petit, C. M.; Ng, L.; Jordan, K. D. *J. Am. Chem. Soc.* **1985**, *107*, 6556–6562.

(8) (a) Sakurai, H.; Nakadaira, Y.; Hosomi, A.; Eriyama, Y.; Kabuto, C. *J. Am. Chem. Soc.* **1983**, *105*, 3359–3360. (b) Sakurai, H.; Eriyama, Y.; Hosomi, A.; Nakadaira, Y.; Kabuto, C. *Chem. Lett.* **1984**, 595–598. (c) Gleiter, R.; Schafer, W.; Sakurai, H. J. *J. Am. Chem. Soc.* **1985**, *107*, 3046–3050.

(9) (a) Dale, J.; Hubert, A. J.; King, G. C. D. *J. Chem. Soc.* **1963**, 73–86. (b) Hubert, A. J.; Dale, J. *J. Chem. Soc.* **1963**, 86–93. (c) Dale, J. *J. Chem. Soc.* **1963**, 93–111. (d) Scott, L. T.; DeCicco, G. J. *Tetrahedron Lett.* **1976**, 2663–2666. (e) Sondheimer, F.; Amiel, Y. *J. Am. Chem. Soc.* **1956**, *78*, 4178–4179. (f) Sondheimer, F.; Amiel, Y. *J. Am. Chem. Soc.* **1957**, *79*, 5817–5820. (g) Sondheimer, F.; Wolovsky, R. *J. Am. Chem. Soc.* **1962**, *84*, 260–269. (h) Sondheimer, F.; Amiel, Y.; Wolovsky, R. *J. Am. Chem. Soc.* **1959**, *81*, 4600–4606. (i) Banerjie, A.; Lando, J. B.; Baughman, R. H. *J. Polym. Sci.* **1979**, *17*, 655–662. (j) Kloster-Jensen, E.; Wirz, J. *Helv. Chim. Acta* **1975**, *58*, 162–177. (k) Cram, D. J.; Allinger, N. L. *J. Am. Chem. Soc.* **1956**, *78*, 2518–2524.

(10) (a) Ittel, S. D.; Ibers, J. A. *Adv. Organomet. Chem.* **1976**, *14*, 33–61. (b) Otsuka, S.; Nakamura, A. *Adv. Organomet. Chem.* **1976**, *14*, 245–283. (c) Mingos, D. M. P. In *Comprehensive Organometallic Chemistry*; Wilkinson, G., Stone, F. G. A., Abel, E. W., Eds.; Pergamon Press: Oxford, 1982; Vol. 3, pp 1–88.

(11) (a) Green, M.; Grove, D.; Howard, J.; Spencer, J.; Stone, F. G. A. *J. Chem. Soc., Chem. Commun.* **1976**, 759–760. (b) Nesmeyanov, A. N.; Gusev, A. I.; Pasynskii, A. A.; Amisimov, K. N.; Kolobova, N. E.; Struchkov, Y. T. *J. Chem. Soc. Chem. Commun.* **1969**, 277–278. (c) Pasynskii, A. A.; Skripkin, Y. V.; Eremenko, I. L.; Kalinnikov, V. T.; Aleksandrov, G. G.; Struchkov, Y. T. *J. Organomet. Chem.* **1979**, *165*, 39–47. (d) Bokiy, N. G.; Gatilov, Y. T.; Struchkov, Y. T.; Ustynyuk, N. A. *J. Organomet. Chem.* **1973**, *54*, 213–219. (e) Cotton, F. A.; Hall, W. T. *J. Am. Chem. Soc.* **1979**, *101*, 5094–5095. (f) Laine, R. M.; Moriarty, R. E.; Bau, R. *J. Am. Chem. Soc.* **1972**, *94*, 1402–1403. (g) Bailey, W. I.; Chisholm, M. H.; Cotton, F. A.; Rankel, L. A. *J. Am. Chem. Soc.* **1978**, *101*, 5764–5773. (h) Churchill, M. R.; Wasserman, H. J. *Inorg. Chem.* **1983**, *22*, 41–44. (i) Maassarani, F.; Pfeffer, M. *J. Am. Chem. Soc.* *106*, 8002–8004. (j) Hey, E.; Weller, F.; Dehnicke, K. *Z. Anorg. Allg. Chem.* **1984**, *514*, 25–38.

(12) Irngartinger, H.; Leiserowitz, L.; Schmidt, G. M. J. *Chem. Ber.* **1970**, *103*, 1119–1131.

(13) (a) Boganovic, B.; Kroner, M.; Wilke, G. *Justus Liebigs Ann. Chem.* **1966**, *699*, 1–23. (b) Jonas, K.; Heimbach, P.; Wilke, G. *Angew. Chem., Int. Ed. Engl.* **1968**, *7*, 949–950. (c) Fischer, K.; Jonas, K.; Wilke, G. *Angew. Chem., Int. Ed. Engl.* **1973**, *12*, 565–566. (d) Mynott, R.; Neidlein, R.; Schwager, H.; Wilke, G. *Angew. Chem., Int. Ed. Engl.* **1986**, *25*, 367–8. (e) Brauer, D. J.; Krüger, C. *J. Organomet. Chem.* **1972**, *44*, 397–402. (f) Jolly, P. W. In *Comprehensive Organometallic Chemistry*; Stone, F. G. A., Ed.; Pergamon Press: New York, 1982; Vol. 8, pp 649–670. (g) Keim, W.; Behr, A.; Röper, M. In *Comprehensive Organometallic Chemistry*; Stone, F. G. A., Ed.; Pergamon Press: New York, 1982; Vol. 8, pp 371–462. (h) Wilke, G. *Angew. Chem., Int. Ed. Engl.* **1988**, *27*, 185–206.

(14) Dietrich, H. *Acta Crystallogr., Sect. B* **1972**, *B28*, 2807–2814.

(15) Fischer, K. Jonas, K.; Mollbach, A.; Wilke, G. *Z. Naturforsch. B* **1984**, *39B*, 1011–1021.

(16) Rösch N.; Hoffman, R. *Inorg. Chem.* **1974**, *13*, 2656–2666.

(17) (a) Ferrara, J. D.; Tessier-Youngs, C.; Youngs, W. J. *J. Am. Chem. Soc.* **1985**, *107*, 6719–21. (b) Ferrara, J. D.; Tessier-Youngs, C.; W. J. *J. Am. Chem. Soc.* **1988**, *110*, 3326–3327.

(18) (a) Day, V. W.; Abdel-Miguid, S. S.; Dabestani, S.; Thomas, M. G.; Pretzer, W. R.; Muetterties, E. L. *J. Am. Chem. Soc.* **1976**, *98*, 8289–8291. (b) Muetterties, E. L.; Pretzer, W. R.; Thomas, M. G.; Beier, B. F.; Thorn, D. L.; Day, V. W.; Anderson, A. B. *J. Am. Chem. Soc.* **1978**, *100*, 2090–2096.

(19) Shriver, D. F. *The Manipulation of Air Sensitive Compounds*; R. E. Krieger Publishing Co.: Malabar, FL, 1982.

(20) NMR were referenced as follows: benzene-d_6, $\delta = 7.15$ ppm (^1H), $\delta = 128.5$ ppm (^{13}C); THF-d_8 $\delta = 1.73$ ppm (^1H), $\delta = 25.3$ ppm (^{13}C); chloroform-*d*, $\delta = 7.24$ ppm (^1H); acetone-d_6, $\delta = 2.09$ ppm (^1H); δ CP-MAS spectra were referenced externally to adamantane (δ 39.5 ppm).

(21) Stephens, R. D.; Castro, C. E. *J. Org. Chem.* **1963**, *28*, 3313–5.

(22) Brandsma, L.; Hommes H.; Verkruijsse, H. D.; de Jong, R. L. P. *Recl. Trav. Chim. Pays-Bas* **1985**, *104*, 226–230.

584 w, 476 w, 462 w cm^{-1} ^1H NMR (chloroform-*d*, AA′BB′ spin system[23]): δ 7.32 (m, 6 H), 7.17 (m, 6 H). ^1H NMR (acetone-d_6, AA′BB′ spin system): δ 7.46 (m, 6 H), 7.34 (m, 6 H). ^1H NMR (benzene-d_6, AA′XX′ spin system): δ 7.20 (m, 6 H), 6.67 (m, 6 H). ^1H NMR (THF-d_8, AA′BB′ spin system: δ 7.33 (m, 6 H), 7.21 (m, 6 H). $^{13}C\{^1H\}$ NMR (benzene-d_6): δ 132.8, 129.1, 127.9, 94.1. $^{13}C\{^1H\}$ NMR (refer to Figure 1 for the numbering scheme for the coupling constants, THF-d_8): δ 132.7 (doublet of doublets of doublets, J_{C4-H4} = 163.0 Hz, J_{C4-H3} = 6.0 Hz, $J_{C4-H4'}$ = 4.2 Hz), 129.1 (doublet of doublets, J_{C3-H3} = 161.0 Hz, J_{C3-H4} = 6.0 Hz), 127.7 (m), 93.6 (d, J_{C1-H3} = 5.7 Hz). ^{13}C CP-MAS: δ 133.2, 129.9, 128.5, 126.6, 94.04.

Synthesis of Ni(TBC). A solution containing 0.8402 g (2.80 × 10^{-3} mol) of TBC in 50 mL of benzene and a solution containing 0.7698 g (2.80 × 10^{-3} mol) of $Ni(COD)_2$ in 40 mL of benzene were combined producing a deep blue-black solution in less than 10 s. The reaction mixture was stirred for several hours, and the volatiles were removed in vacuo leaving a blue-black powder. Yield: 1.0097 g, 99.9%. The Ni(TBC) was purified further by recrystallization from benzene to remove any trace of Ni metal (from $Ni(COD)_2$) and TBC. IR (Nujol, KBr): 3074 w, 1983 m, 1963 sh, 1957 s, 1550 w, 1488 w, 1460 m, 1438 w, 1279 w, 1135 w, 759 s, 743 s, 575 m, 506 m, 483 m cm^{-1}. ^1H NMR (C_6D_6, AA′XX′ spin system[23]): δ 7.57 (m, 6 H), 6.79 (m, 6 H). ^1H NMR (THF-d_8, AA′XX′ spin system[23]): δ 7.78 (m, 6 H), 7.23 (m, 6 H). $^{13}C\{^1H\}$ NMR (C_6D_6): δ 142.9, 130.6, 128.6, 109.6. ^{13}C NMR (THF-d_8): δ 142.7 (m), 130.5 (sextet (doublet of doublets of doublets)), J_{CH} = 161.1 Hz, J_{CCH} = 4.7 Hz), 128.0 (quartet, J_{CH} = 161.9 Hz, J_{CCH} = 7.7 Hz), 109.6 (doublet, J_{CH} = 5.2 Hz). ^{13}C CP-MAS: δ 142.7, 133.0, 128.0, 112.0. FDMS: 358.2 (5) amu. UV–vis: 587.5 (ϵ = 2.5 × 10^3), 370 nm ($\epsilon \simeq 10^3$). Anal. Calcd for $NiC_{24}H_{12}$: C, 80.3; H, 3.37. Found: C, 79.5; H, 3.25.

Reactions of Ni(TBC) with Small Molecules. The complex Ni(TBC) was combined with carbon monoxide in THF, Et_2O, and benzene. The following procedure was used for all three solvents. A 30-mL two-neck flask was charged with 0.010 g (2.8 × 10^{-5} mol) of Ni(TBC). The solid was dissolved in 15 mL of the solvent and carbon monoxide gas bubbled through the solution. The period of reaction was defined as the time interval from the start of bubbling until the solution was clear yellow. The reaction rates with oxygen were determined in a similar fashion. The reactions of Ni(TBC) with other small molecules were monitored by NMR. The following combinations of solvents and/or reagents were vacuum transferred to NMR tubes which contained approximately 5 mg of Ni(TBC): 0.5 mL of C_6D_6 and 0.05 mL of CH_3CN, 0.5 mL of C_6D_6 and 0.1 mL of H_2O, and 0.5 mL of $CDCl_3$. For reaction with CO_2, the gas (Airco) was bubbled into a solution of Ni(TBC) in C_6D_6. The NMR tube was flame sealed and the ^1H NMR recorded.

Electrochemical Measurements. A three-compartment electrochemical cell (~15 mL capacity) was used for electrochemical measurements. A coiled Pt wire was used as a counter electrode and separated from the working electrode compartment by a glass frit. The reference electrode was lithium foil immersed in a solution 0.1 M $LiBF_4$ in THF. The working electrode used for cyclic voltammetry experiments was a cylindrically shaped Pt wire (diameter = 1 mm, area = 0.3 cm^2). Solutions of TBC and Ni(TBC) were prepared as 1.0 × 10^{-3} M in 0.10 M TBAP in THF. Ferrocene (2.68 × 10^{-3} M in 0.10 M TBAP in THF) was used as a reference. All the electrochemical measurements were carried out at room temperature under an argon atmosphere in a Vacuum Atmospheres Corp. (VAC-HE 493 Dry Train) drybox. Oxygen and moisture levels in the drybox were usually less than 1 ppm and monitored continuously by a MA-1 (VAC) moisture analyzer and a 317BX Teledyne oxygen analyzer. A PARC Model 176 potentiostat coupled with a PARC Model 175 universal programmer and a Yokogawa Model 3036 recorder were used to monitor the electrochemical measurements.

Conductivity Measurements. Conductivity measurements were made in a two-probe device designed in this laboratory.[24] Measurements were made by compacting finely ground powder to approximately 2 × 10^3 psi and measuring the resistance across the compacted disk. A minimum of four resistance measurements were recorded for each sample ranging in thickness from 0.5 to 5.0 mm, and the derived conductivities were averaged.

Oxidation of Ni(TBC) with I_2. Method A. Ni(TBC) (0.020 g, 5.57 × 10^{-5} mol) was ground in a mortar along with I_2 (0.023 g, 1.18 × 10^{-4} mol) in a glovebag under argon. Several drops of Et_2O were added repeatedly, to dissolve the I_2, and allowed to evaporate. Conductivity: less than 7.15 × 10^{-7} (Ω cm^{-1}). IR (Nujol): 1983 vw, 1957 vw, 1487 m, 950 w, 755 s cm^{-1}. **Method B.** A two-compartment flask with a valve between compartments was assembled. One flask was charged with 0.033 g of Ni(TBC) (9.00 × 10^{-5} mol) and the other flask with 0.0117 g of I_2 (4.61 × 10^{-5} mol) under an argon atmosphere. The valve was opened and the I_2 vapor allowed to diffuse into the flask containing the Ni(TBC). The reaction was terminated after all the I_2 vapor had disappeared (4 days). Conductivity: less than 7.15 × 10^{-7} (Ω-cm^{-1}). IR (Nujol): 2215 vw, 1954 m, 1956 m, 1549 w, 1485 s, 1277 w, 951 w, 945 w, 869 w, 857 w, 755 s, 574 s, 506 s, 482 s cm^{-1}. **Method C.** A flask was charged with 0.029 g of Ni(TBC) (8.08 × 10^{-5} mol) and 0.0103 g of I_2 (8.12 × 10^{-5} mol). Approximately 15 mL of freshly distilled Et_2O was added, and the solution was stirred for 1 h. The solvent was removed in vacuo. Conductivity: less than 7.15 × 10^{-7} (Ω cm^{-1}). IR (Nujol): 2216 vw, 1983 w, 1964 m, 1957 m, 1486 s, 754 vs, 751 vs, 575 w, 475 w cm^{-1}.

Alkali-Metal Reduction of Ni(TBC). General Procedures. Argon for Schlenk techniques was purified by passing through a 7 cm × 30 cm column of Ridox (40%) and 4-Å molecular sieves (60%). The atmosphere in the drybox (Vacuum Atmospheres Corp. HE-493) was maintained below 1 ppm of O_2 as measured by a Teledyne 317BX oxygen analyzer. Argon for the drybox was prepurified by passage through a GE Go-Getter to reduce O_2 and H_2O to less than 0.1 ppm in the incoming stream. All the reduction products synthesized react with Teflon; therefore, care was taken to assure that the solutions came into contact only with dry glass or reduced Teflon. The number of joints in the apparatus was minimized.

Reduction of Ni(TBC) with Lithium. The complex Ni(TBC) was combined with lithium sand in the solvents: THF, dimethoxyethane (DME), and THF containing a stoichiometric amount of TMEDA (2 equiv of TMEDA/Ni(TBC)). A 100-mL flask equipped with a frit was charged with 0.050 g of Ni(TBC) (1.4 × 10^{-4} mol) and 0.003 g of Li sand (4.3 × 10^{-4} mol) and 30 mL of THF, stirred 5.5 h, and filtered through a medium frit. The THF was removed in vacuo. The product was ground into a fine powder, and conductivity measurements were performed. Attempts to obtain crystals by slow removal of THF or DME were unsuccessful. IR (Nujol): $Li_x[Ni(TBC)]\cdot n$THF ($x \geq 1.5$), 1881 m, 1843 m, 1817 m, 1542 m, 1368 s, 1350 w, 1289 w, 1131 s, 1040 s, 986 m, 913 m, 812 m, 452 w cm^{-1}; $Li_x[Ni(TBC)]\cdot$nDME, decomposed; $Li_x[Ni(TBC)]\cdot n$TMEDA ($x \simeq 1$):[25a] 1960 w (br), 1873 (br), 1540 m, 1506 s, 1410 s, 1356 s, 1321 s, 1300 s, 1288 s, 1261 s, 1247 s, 1221 s, 1183 s, 1157 s, 1131 s, 1098 s, 1064 s, 1031 s, 1019 s, 1006 s, 946 m, 823 m, 801 m, 788 m, 752 s (br), 734 s (br) cm^{-1}.

The above $Li_x[Ni(TBC)]\cdot n$THF (0.020 g) was dissolved in 20 mL of THF which contained Ni(TBC) (0.029 g) to give ~ 0.3e/Ni(TBC) and the THF was removed in vacuo. IR (Nujol): 1983 w, 1957 m, 1870 m (br), 1504 w, 1409 m, 1368 w, 1342 w, 1318 w, 1287 w, 1280 w, 1217 w (br), 759 s, 753 s, 742 s, 574 m, 505 w, 482 w cm^{-1}. Conductivity: σ = 7.2 (7) × 10^{-5} (Ω cm)$^{-1}$.

Reduction of Ni(TBC) with Sodium in the Presence of C222. A flask equipped with a frit and a collection flask was charged with 0.100 g (2.78 × 10^{-4} mol) of Ni(TBC), 0.210 g (5.58 × 10^{-4} mol) of C222, 0.016 g (6.96 × 10^{-4} mol) of Na, and 70 mL of freshly distilled THF and stirred 24 h. The THF solution turned from blue to purple in a few minutes. The soluble components were separated from the insoluble components by filtration through a medium frit. After removal of the solvent in vacuo 0.200 g of a THF insoluble purple solid and 0.029 g of a THF-soluble purple solid were isolated. IR (Nujol) of the THF insoluble product: 1876 s (br), 1834 s, 1540 w, 1529 w, 1504 s,

---

[23] For a discussion of AA′XX′ spin systems see: Bovey, F. A. *Nuclear Magnetic Resonance Spectroscopy*; Academic Press: New York, 1969; pp 117–127.

[24] The minimum conductivity that may be measured in our device is 7.15 × 10^{-7} (Ω cm)$^{-1}$.

[25] (a) The values of *x* in these samples was estimated from the ratio of the intensities of the monoanion and dianion C≡C infrared stretches. (b) Infrared data indicated the presence of a trace of the monoanion.

1410 s, 1365 m, 1349 s, 1320 m, 1301 m, 1290 s, 1265 s, 1222 m, 1198 m, 1176 w, 1159 w, 1131 s, 1100 s (br), 1004 m, 982 m, 928 m (br), 823 m, 811 m, 710 m, 449 w cm^{-1}. IR (Nujol) of the THF-soluble product: 1877 m, 1856 w, 1537 w, 1504 m, 1411 m, 1365 m, 1326 m, 1301 m, 1272 m, 1223 m, 1174 m, 1132 s (br), 1101 s, 1090 s, 1072 s, 1056 m, 1037 m, 1018 m, 996 m, 982 s, 922 m, 850 w, 832 w, 823 m, 761 w, 732 m, 581 w, 476 w, 462 w (br) cm^{-1}.

Reduction of Ni(TBC) with Potassium in the Presence of 18-Crown-6. A flask equipped with a frit and a collection flask was charged with 0.190 g (5.51×10^{-4} mol) of Ni(TBC), 0.360 g (1.36×10^{-3} mol) of 18-crown-6, and 0.061 g (1.56×10^{-3} mol) of potassium. After 30 mL of THF was added to the mixture, it was stirred for 24 h. The mixture was filtered and cooled to −78 °C overnight, resulting in the formation of a purple solid. The mother liquor was filtered off through a second frit, and the volatiles were removed in vacuo. Yield: 0.360 g of $[K(18\text{-crown-}6)]_x[Ni(TBC)]$ ($x \sim 1.5$). IR (Nujol): 1870 w (br), 1851 m, 1824 m, 1535 w, 1505 m, 1410 m, 1351 s, 1321 m, 1290 m, 1250 m, 1222 m, 1199 m, 1131 s (br), 1108 s, 1003 m, 960 m, 864 w, 856 w, 838 mw, 823, w, 812 w, 712 w cm^{-1}. The IR data for the mother liquor solids (Nujol): 2112 w, 2089 w, 2070 w, 2030 w, 1976 w, 1926 w, 1877 m, 1847 m, 1828 m, 1731 w, 1575 m, 1535 w, 1506 m, 1365 s, 1351 vs, 1325 m, 1291 s, 1251 s, 1223 m, 1200 m, 1118 vs, 1111 vs, 1002 m, 997 m, 985 s, 962 s, 905 w, 839 s, 825 m, 812 m, 730 s, 714 s, 534 w cm^{-1}. An NMR experiment was performed as follows: nonstoichiometric amounts of Ni(TBC), 18-crown-6, and potassium were placed in an NMR tube equipped with a valve and a joint. Approximately 0.5 mL of THF was distilled into the tube, and the NMR tube was flame sealed. The sample was kept at −196 °C until the spectra were recorded. The ^1H NMR spectra were recorded in the range ±120 ppm relative to TMS.

Reduction of Ni(TBC) with Potassium in the Presence of C222. A flask equipped with a frit and a collection flask was charged with 0.100 g (2.78×10^{-4} mol) of Ni(TBC), 0.210 g (5.58×10^{-4} mol) of C222, and 0.027 g (6.90×10^{-4} mol) of potassium and 70 mL of freshly distilled THF. The solution was initially deep blue. The color turned deep purple over the next 2 h and turned red-brown after 6 h. No further color change was noted after 24 h. The reaction mixture was filtered, and all but 3–4 mL of THF was removed from the filtrate by vacuum distillation. The mother liquor was filtered back into the reaction flask, the solid was washed with two 2-mL portions of THF, and the remaining solvent was removed in vacuo. Yield: 0.252 g of a black-brown amorphic solid, $[K(C222)]_2[Ni(TBC)]$,[25b] 76% based on Ni(TBC). IR (Nujol): 1873 w, 1830 ms, 1582 w, 1526 w, 1506 w, 1412 w, 1360 m, 1349 s, 1323 w, 1290 s, 1258 m, 1242 w, 1198 m, 1173 w, 1130 s, 1104 s, 1081 s, 1029 w, 980 m, 948 ms, 935 m, 903 w, 831 ww, 821 w, 811 m, 783 w, 774 w, 752 w, 712 m, 523 w, 451 w cm^{-1}. The ^1H NMR (±220 ppm) and EPR spectra of this sample was recorded in THF-d_8 and THF, respectively. Conductivity: $\sigma = 1.6 \times 10^{-7}$ $(\Omega\ cm)^{-1}$.

Doping of Ni(TBC) with $[K(C222)]_2[Ni(TBC)]$. The following procedure was used for all doping reactions. Ni(TBC) and $[K(C222)]_2[Ni(TBC)]$ were combined in the appropriate stoichiometries to give ~0.050 g of final product. The stoichiometries used are shown by the abscissa in the plot in Figure 6 [number of electrons per TBC unit = 2(mol of dianion)/(mol of dianion + mol of neutral)]. The solids were dissolved in 20 mL of freshly distilled THF and stirred for 10–15 min and the volatiles removed in vacuo at room temperature. Each sample was measured for conductivity (Figure 7), and an IR (Nujol) spectrum was recorded.

Reduction of TBC with Potassium and C222. A flask equipped with a frit and a collection flask was charged with 0.100 g of TBC (3.33×10^{-4} mol), 0.251 g of C222 (6.66×10^{-4} mol), 0.033 g of potassium (8.32×10^{-4} mol) and 70 mL of THF and stirred. The color of the solution was initially pale yellow. The solution turned pale blue rapidly. The blue color deepened over 2 h, and finally the solution turned blue-green after approximately 6 h. No further color changes was noted after 24 h. The reaction mixture was filtered, and all but 3–4 mL of THF was removed by vacuum distillation. The mother liquor was filtered back into the reaction flask, and the remaining solvent was removed in vacuo. Yield: 0.280 g of a black-blue amorphic solid, $[K(C222)]_2(TBC)$, 74% based on TBC. Yield of mother liquor solid: 0.032 g. Infrared spectra were recorded for both products and the conductivity of the former was measured. $[K(C222)]_2(TBC)$: IR (Nujol) 2089 w, 2036 m, 2000–1900 vw (br), 1800–1700 vw (br), 1626 w, 1584 m, 1544 w, 1522 w, 1501 w, 1404 m, 1397 m, 1354 s, 1322 s, 1298 s, 1273 s, 1260 s, 1236 s, 1194 s, 1174 w, 1132 s, 1102 s, 1079 s, 1030 m, 994 m, 949 s, 933 s, 903 w, 831 w, 819 w, 808 m, 750 m, 472 w cm^{-1}. The IR (Nujol) of the mother liquor solids showed very weak TBC bands and strong C222 bands.

Table I. Crystal Data, Data Collection and Reduction, and Refinement Details for the Crystal Structure of Ni(TBC)

formula	$Ni(C_{24}H_{12})$
f wt	359.07 amu
temp	23 °C
space group	*Pna*2_1
cell	
a	15.518 (3) Å
b	18.761 (4) Å
c	5.375 (1) Å
V	1564.8 (5) $Å^3$
Z	4
D(calcd)	1.528 (1) g cm^{-3}
D(obsd)	1.54 (1) g cm^{-3}
cryst faces, dimens (mm)	{−1,−1,0}, 0.100; {1,−1,0}, 0.110; {0,0,1}, 0.200
cryst volume	2.20×10^{-3} mm^3
diffractometer	Syntex $P2_1$
radiation	Mo Kα (0.71073 Å)
monochromator	highly oriented graphite crystal
scan type	$2\theta-\theta$
scan speed	3.91° min^{-1} (2θ)
scan range	1.0° below Kα_1 to 1.0° above Kα_2
bkgnd scan	the cryst and detector were held stationary at the beginning and the end of the scan, each for one-half the total scan time
2θ scan limits	$3.0° \leq 2\theta \leq 55.0°$
std reflctns	6 every 94 reflctns
indices	(0 0 4), (0 9 1), (8 0 2), (5 1 2), (0 3 3), (9 6 0)
cryst stability	no indication of check reflctn decay during data collectn
total reflctns scanned	2129
unique reflctns ($I \geq 3\sigma(I)$)	828
unique reflctns ($I \geq 0$)	1667
abs correctn	numerical (UCLA Package)
linear abs coeff	12.444 cm^{-1}
transmissn factor range	0.873–0.895
scattering factor source	International Tables (UCLA Package)
hydrogen atom treatment	ideal positions were calculated at 0.9500 Å with the *B* value set to 1 $Å^2$ greater than the isotropic *B* value of the carbon which the hydrogen is bonded
parameters refined (*F*)	105
$R(F)^a$	0.112
$R_w(F)^a$	0.061
goodness of fit $(F)^a$	1.09
$R(F)^b$	0.046
$R_w(F)^b$	0.044
shift/esd ratio	≤0.01
correct crystal chirality determined	

[a] $F_\sigma^2 \geq 0$. [b] $F_\sigma^2 \geq 3\sigma(F_\sigma^2)$.

Doping of TBC with $[K(C222)]_2(TBC)$. The same procedure was followed for this experiment as with Ni(TBC).

X-ray Analysis. Crystals of Ni(TBC) were grown by slow concentration of a benzene solution. A crystal was mounted on a glass fiber and the unit cell determined on a Syntex $P2_1$ diffractometer by least-squares refinement of the indices and angles of 15 reflections with $20.0° \leq 2\theta \leq 30.0°$. Crystal data, data collection and reduction, and structure refinement details are given in Table I. The *mmm* symmetry and the systematic absences ($0kl$, $k + l = 2n + 1$; $h0l$, $h = 2n + 1$; $00l$, $l = 2n + 1$) of the diffraction data indicated the space group was either *Pnam* or *Pna*2_1. The structure was successfully solved and refined in *Pna*2_1. The density of the crystal was determined by flotation in aqueous CsI. The position of the nickel atom was determined by direct methods.[26] The positions of the carbon atoms were found by

Table II. Final Positional Parameters for Nickel and Carbon in Ni(TBC)

atom	*x/a*	*y/b*	*z/c*
Ni	0.30236 (6)	0.03666 (6)	0.00000
C(01)	0.2837 (5)	−0.0661 (4)	0.0564 (17)
C(02)	0.2404 (5)	−0.0304 (5)	0.2107 (18)
C(03)	0.1855 (6)	0.0010 (5)	0.3909 (20)
C(04)	0.1863 (6)	0.0756 (5)	0.3946 (18)
C(05)	0.2430 (6)	0.1081 (5)	0.2078 (20)
C(06)	0.2873 (6)	0.1388 (5)	0.0500 (23)
C(07)	0.3325 (6)	0.1837 (5)	−0.1222 (19)
C(08)	0.3802 (6)	0.1459 (5)	−0.2980 (21)
C(09)	0.3745 (7)	0.0680 (6)	−0.2778 (22)
C(10)	0.3754 (6)	0.0028 (6)	−0.2710 (22)
C(11)	0.3760 (6)	−0.0730 (5)	−0.3006 (22)
C(12)	0.3296 (6)	−0.1121 (5)	−0.1194 (18)
C(13)	0.1354 (5)	−0.0366 (6)	0.5665 (17)
C(14)	0.0854 (6)	0.0008 (6)	0.7381 (22)
C(15)	0.0854 (6)	0.0756 (5)	0.7313 (22)
C(16)	0.1360 (6)	0.1120 (5)	0.5663 (19)
C(17)	0.3352 (6)	0.2596 (5)	−0.1221 (21)
C(18)	0.3815 (7)	0.2942 (5)	−0.3079 (20)
C(19)	0.4265 (5)	0.2551 (5)	−0.4924 (33)
C(20)	0.4261 (5)	0.1816 (4)	−0.4868 (34)
C(21)	0.4221 (5)	−0.1099 (4)	−0.4902 (34)
C(22)	0.4181 (5)	−0.1834 (4)	−0.4989 (35)
C(23)	0.3702 (7)	−0.2211 (5)	−0.3215 (21)
C(24)	0.3259 (6)	−0.1853 (5)	−0.1300 (20)

Table III. Bond Lengths (Å) for Nickel and Carbon in Ni(TBC)

from	to	dist	from	to	dist
Ni	C(01)	1.974 (8)	C(08)	C(09)	1.468 (12)
Ni	C(02)	1.946 (9)	C(08)	C(20)	1.409 (17)
Ni	C(05)	1.972 (10)	C(09)	C(10)	1.225 (11)
Ni	C(06)	1.948 (9)	C(10)	C(11)	1.430 (11)
Ni	C(09)	1.957 (12)	C(11)	C(12)	1.416 (14)
Ni	C(10)	1.952 (12)	C(11)	C(21)	1.424 (17)
C(01)	C(02)	1.260 (12)	C(12)	C(24)	1.375 (13)
C(01)	C(12)	1.464 (12)	C(13)	C(14)	1.395 (13)
C(02)	C(03)	1.418 (13)	C(14)	C(15)	1.404 (12)
C(03)	C(04)	1.400 (11)	C(15)	C(16)	1.368 (13)
C(03)	C(13)	1.411 (12)	C(17)	C(18)	1.391 (13)
C(04)	C(05)	1.467 (13)	C(18)	C(19)	1.417 (16)
C(04)	C(16)	1.388 (12)	C(19)	C(20)	1.380 (11)
C(05)	C(06)	1.234 (13)	C(21)	C(22)	1.381 (11)
C(06)	C(07)	1.435 (13)	C(22)	C(23)	1.400 (17)
C(07)	C(08)	1.394 (13)	C(23)	C(24)	1.408 (13)
C(07)	C(17)	1.426 (13)			

successive difference Fourier syntheses, and the model was refined by full-matrix least-squares refinement. The *z* coordinate of the nickel atom was fixed at 0.0000. The hydrogen atoms were placed at ideal positions after each refinement (d_{C-H} = 0.95 Å and a *B* value 1 Å^2 greater than the carbon to which it was bonded).[27] An analytical absorption correction was applied to the data. The nickel atom was refined anisotropically, and the carbon atoms were refined isotropically so as to maintain an acceptable data to parameter ratio. The final *R* values for the 848 data with $I \geq 3\sigma(I)$ are $R(F) = 0.046$ and $R_w(F) = 0.044$. The correct crystal chirality was determined by refining the two possible chiral models to convergence and choosing the one that gave the lower residuals. Final positional parameters, bond distances, and bond angles for the non-hydrogen atoms are given in Tables II, III, and IV, respectively.

ASED-MO Calculations. ASED-MO calculations on Ni(TBC) were performed by using the parameters[28] given in Table sIV of the supplementary material. Calculations were based on ideal D_{3h} symmetry by using the crystallographically determined bond lengths and angles for the geometry.

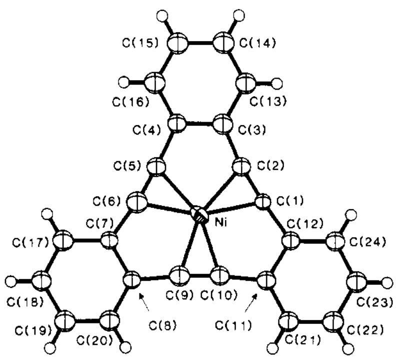

Figure 1. ORTEP labeling diagram of Ni(TBC). The thermal ellipsoids are drawn at 50% probability level, and the hydrogen atoms are drawn arbitrarily small for clarity.

Results and Discussion

Synthesis of Ni(TBC). Ni(TBC) is obtained quantitatively from the reaction of Ni(COD)$_2$ with TBC in benzene. It has been established that Ni(COD)$_2$ is thermally unstable and the COD ligands are quite labile.[13a] This type of ligand exchange reaction has been well characterized for many COD complexes.[11a,29,30] The use of freshly sublimed Ni(COD)$_2$ is important to the success of the reaction. Impure Ni(COD)$_2$ readily forms a nickel mirror destroying the stoichiometry of the reaction. This decomposition has been shown to proceed catalytically from trace peroxides.[18a] The use of toluene rather than benzene as solvent led to incomplete reaction.

Description of the Structure of Ni(TBC). The overall geometry of Ni(TBC) (Figure 1) can be described as trigonal planar with the Ni atom in the center of the TBC ligand, coordinated by three alkynes with Ni–alkyne carbon distances averaging 1.958 (5) Å. Bond distances and angles are tabulated in Tables III and IV. The Ni–C distance is considerably shorter than the Cu–C distance (2.060 (4) Å) in the isoelectronic Cu(TBC)(OTf).[31] The C≡C—C linkages (C(01)—C(02)—C(03)) are distorted from linearity with C≡C—C angles averaging 173.8 (9)° compared to 178.3 (9)° for free TBC[12,31] and 177.8 (6)° in Cu(TBC)(OTf).[31] The alkyne carbon–carbon bond length in the complex is 1.240 (10) Å compared with 1.192 (2) Å in free TBC and 1.222 (10) Å in Cu(TBC)(OTf). The metal atom in Ni(TBC) is 0.338 (8) Å above the least-squares plane defined by the six alkyne carbons (root-mean-square deviation = 0.013 Å) as compared to 0.1809 (9) Å in Cu(TBC)(OTf). The least-squares plane defined by all 24 carbons of the TBC ligand (root-mean-sequence deviation = 0.060 Å) indicates the molecule is nearly planar. The overall geometry of Ni(TBC) is distorted from ideal D_{3h} symmetry by a slight bending downward of all three benzo groups. The dihedral angles of the planes of the benzo groups with respect to the plane of the six alkyne carbons

---

(26) (a) Main, P.; Lessinger, L.; Woolfson, M. M.; Germain, G.; Declercq, J. P. MULTAN76, A System of Computer Programs for the Automatic Solution of Crystal Structures from X-ray Diffraction Data; Universities of York and Louvain: York, England, and Louvain, Belgium, 1976. (b) The UCLA Crystallographic Computing Package, Jan 5, 1982.

(27) Churchill, M. R. *Inorg. Chem.* **1973**, *12*, 1213–14.

(28) (a) Anderson, A. B. *J. Chem. Phys.* **1976**, *65*, 206. (b) Anderson, A. B. *J. Chem. Phys.* **1977**, *66*, 5108.

(29) (a) Boag, N. M.; Green, M.; Grove, D. M.; Howard, J. A. K.; Spencer, J. L.; Stone, F. G. A. *J. Chem. Soc., Dalton Trans.* **1980**, 2170–81. (b) Boag, N. M.; Green, M.; Howard, J. A. K.; Spencer, J. L.; Stansfield, R. F. D.; Thomas, M. D. O.; Stone, F. G. A.; Woodward, P. *J. Chem. Soc., Dalton Trans.* **1980**, 2182–90. (c) Boag, N. M.; Green, M.; Howard, J. A. K.; Stone, F. G. A.; Wadepohl, H. *J. Chem. Soc., Dalton Trans.* **1980**, 2170–81.

(30) (a) English, A. D.; Jesson, J. P.; Tolman, C. A. *Inorg. Chem.* **1976**, *7*, 1730–1732. (b) Jonas, K.; Schieferstein, L. *Angew. Chem., Int. Ed. Engl.* **1979**, *7*, 549–550. (c) Green, M.; Kuc, T. A.; Taylor, S. H. *J. Chem. Soc., Inorg. Phys. Theor.* **1971**, 2334–2337.

(31) Ferrara, J. D.; Tessier-Youngs, C.; Youngs, W. J. *Organometallics* **1987**, *6*, 676–678.

Table IV. Bond Angles (deg) for Nickel and Carbon in Ni(TBC)

from	through	to	angle	from	through	to	angle
C(01)	Ni	C(02)	37.5 (4)	C(05)	C(06)	C(07)	171.7 (10)
C(01)	Ni	C(05)	120.4 (4)	C(06)	C(07)	C(08)	113.5 (8)
C(01)	Ni	C(06)	157.2 (3)	C(06)	C(07)	C(17)	126.9 (9)
C(01)	Ni	C(09)	119.7 (4)	C(08)	C(07)	C(17)	119.5 (10)
C(01)	Ni	C(10)	83.2 (4)	C(07)	C(08)	C(09)	115.0 (10)
C(02)	Ni	C(05)	83.0 (4)	C(07)	C(08)	C(20)	121.0 (9)
C(02)	Ni	C(06)	119.7 (4)	C(09)	C(08)	C(20)	123.8 (10)
C(02)	Ni	C(09)	157.0 (4)	Ni	C(09)	C(10)	71.5 (9)
C(02)	Ni	C(10)	120.7 (5)	Ni	C(09)	C(08)	113.0 (8)
C(05)	Ni	C(06)	36.7 (4)	C(10)	C(09)	C(08)	175.2 (14)
C(05)	Ni	C(09)	119.7 (5)	Ni	C(10)	C(09)	72.0 (9)
C(05)	Ni	C(10)	156.2 (5)	Ni	C(10)	C(11)	114.2 (9)
C(06)	Ni	C(09)	83.0 (5)	C(09)	C(10)	C(11)	171.9 (16)
C(06)	Ni	C(10)	119.5 (5)	C(10)	C(11)	C(12)	115.8 (11)
C(09)	Ni	C(10)	36.5 (3)	C(10)	C(11)	C(21)	124.4 (11)
Ni	C(01)	C(02)	70.1 (6)	C(12)	C(11)	C(21)	119.8 (10)
Ni	C(01)	C(12)	113.8 (6)	C(01)	C(12)	C(24)	126.4 (9)
C(02)	C(01)	C(12)	175.8 (9)	C(11)	C(12)	C(24)	120.6 (10)
Ni	C(02)	C(01)	72.4 (6)	C(01)	C(12)	C(11)	112.8 (8)
Ni	C(02)	C(03)	115.2 (7)	C(03)	C(13)	C(14)	119.8 (10)
C(01)	C(02)	C(03)	172.0 (10)	C(13)	C(14)	C(15)	119.1 (11)
C(02)	C(03)	C(04)	114.8 (10)	C(14)	C(15)	C(16)	121.0 (11)
C(02)	C(03)	C(13)	125.5 (9)	C(04)	C(16)	C(15)	120.6 (10)
C(04)	C(03)	C(13)	119.7 (10)	C(07)	C(17)	C(18)	118.8 (10)
C(03)	C(04)	C(05)	114.3 (10)	C(17)	C(18)	C(19)	121.0 (9)
C(03)	C(04)	C(16)	119.8 (10)	C(18)	C(19)	C(20)	120.0 (14)
C(05)	C(04)	C(16)	126.0 (9)	C(08)	C(20)	C(19)	119.5 (14)
Ni	C(05)	C(06)	70.6 (6)	C(11)	C(21)	C(22)	119.1 (13)
Ni	C(05)	C(04)	112.7 (7)	C(21)	C(22)	C(23)	120.4 (14)
C(06)	C(05)	C(04)	176.2 (10)	C(22)	C(23)	C(24)	121.0 (10)
Ni	C(06)	C(05)	72.7 (6)	C(12)	C(24)	C(23)	119.1 (10)
Ni	C(06)	C(07)	115.4 (7)				

are in the range 1.9–3.9°. The remainder of the TBC ligand is not distorted from the geometry of free TBC with the exception of the angles around the ipso carbons of the benzene ring. The mean angle for C(alkyne)–C(ipso)–C(β), i.e. C(02)–C(03)–C(13), is 125.5 (12)° and 120.7 (3)° in Ni(TBC) and TBC, respectively. The mean angle for C(alkyne)–C(ipso)–C(ipso), i.e. C(02)–C(03)–C(04)), is 114.4 (11)° in Ni(TBC) and 119.0 (3)° in TBC. These structural changes of the TBC ligand in Ni(TBC) are consistent with the bend of the C≡C bond toward the nickel atom. The mean C–C (C(01)–C(12)) single bond length and C⋯C aromatic bond length are 1.447 (22) and 1.399 (17) Å for Ni(TBC) and 1.434 (2) and 1.387 (13) Å for TBC.[12] The mean bond angles in the benzene rings are 120.1 (6) and 119.0 (3) in Ni(TBC) and TBC, respectively.

The molecular structure of Ni(TBC) shows a relatively small distortion of the C≡C bond compared to the structures of (1,2-μ_2-diphenylethyne)[1,2-bis(dimethylphosphino)ethane-*P*,*P*′]nickel(0)[32] (1) and bis(*tert*-butyl isocyanide)(1,2-μ_2-diphenylethyne)nickel(0)[33] (2). The Ni—C and C≡C bond lengths and C≡C—C angles for complexes 1 and 2 are listed in Table V along with the values for Ni(TBC). Inspection of Table V shows that the Ni–C bond lengths in Ni(TBC) (1.958 (5) Å) are longer than those in complexes 1 and 2 (1.878 (2) and 1.899 (19) Å, respectively). The C≡C bond in Ni(TBC) (1.240 (10) Å) is considerably shorter than the C≡C bond length in complexes 1 and 2 (1.28 (2) and 1.290 (3) Å, respectively), whereas the C≡C—C bond angle is much greater (173.8 (9)° in Ni(TBC) and 146.0 (6) and 149 (1)° in 1 and 2, respectively). Many diphenylethyne complexes have much larger distortions of the C≡C—C linkage.[10,17] Two structures in which the metal centers bind to the alkynes of TBC above the plane have been determined.[34,35] In these structures the bending occurs perpendicular to the TBC plane showing that significant deformation is possible for out-of-plane coordination.

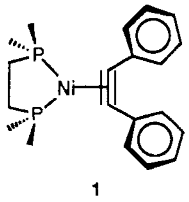

1

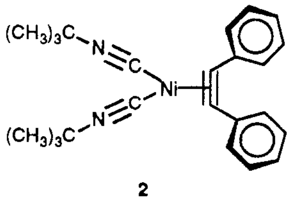

2

Table V. Comparisons of Relevant Bond Lengths (Å) and Angles (deg) in TBC, Ni(TBC), Cu(TBC)(OTf), 1 and 2.

compd	ref	M—C	C≡C	C≡C—C
TBC	12	2.08^{a,b}	1.192 (2)	178.3 (9)
Ni(TBC)	this work	1.958 (5)	1.240 (10)	173.8 (9)
Cu(TBC)(OTf)	30	2.060 (4)	1.222 (10)	177.8 (6)
1	32	1.878 (2)	1.290 (3)	146.0 (6)
2	33	1.899 (19)	1.28 (2)	149 (1)

^{a}This represents the distance of the alkyne carbons to the centroid of the 12-membered ring. ^{b}This value was calculated from data in the reference.

It has been suggested that the metal–carbon bond length in a given series of complexes is a better indicator of the relative strength of the π-alkyne transition metal interaction than the C≡C bond length.[10a,36] The long Ni—C and short C≡C bond lengths and larger C≡C—C angle

---

[32] Pörschke, K. R.; Mynott, R.; Angermund, K.; Krüger, C. *Z. Naturforsch., B* **1985**, *40B*, 199–209.

[33] Dickson, R. S.; Ibers, J. A. *J. Organomet. Chem.* **1972**, *36*, 191–207.

[34] Ferrara, J. D.; Tessier-Youngs, C.; Youngs, W. J. *Inorg. Chem.* **1988**, *27*, 2201–2202.

[35] Djebli, A.; Ferrara, J. D.; Tessier-Youngs, C.; Youngs, W. J. *J. Chem. Soc., Chem. Commun.* **1988**, 548–549.

[36] (a) Nelson, J. H.; Wheelock, K. S.; Cusachs, L. C.; Jonassen, H. B. *J. Am. Chem. Soc.* **1969**, *91*, 7005–8. (b) Tatsumi, K.; Hoffman, R.; Templeton, J. L. *Inorg. Chem.* **1982**, *21*, 466–68. (c) Greaves, E. O.; Lock, C. J. L.; Maitlis, P. M. *Can. J. Chem.* **1968**, *46*, 3879–3891. (d) Nelson, J. H.; Wheelock, K. S.; Cusachs, L. C.; Jonassen, H. B. *J. Chem. Soc., Chem. Commun.* **1969**, 1019–1020.

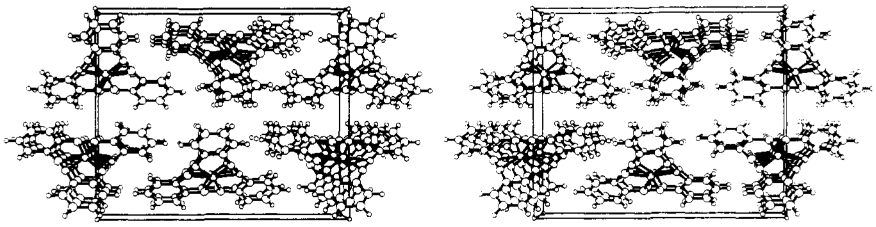

Figure 2. ORTEP stereoview of Ni(TBC) looking down the *c* axis with the *b* axis to the right. The thermal ellipsoids are drawn at 50% probability level except for the hydrogen atoms which are drawn arbitrarily small for clarity.

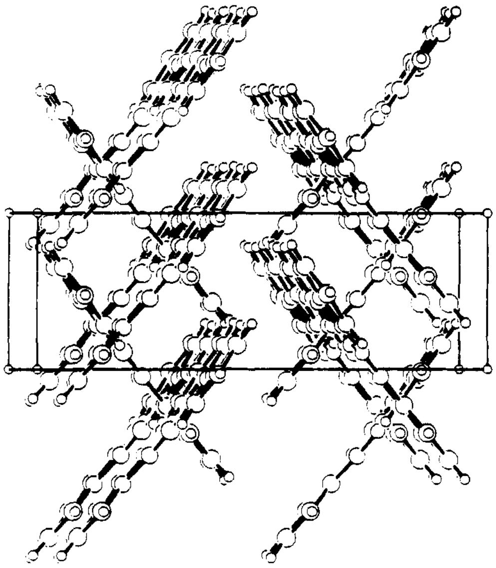

Figure 3. ORTEP packing diagram of Ni(TBC) looking down the *b* axis with the *a* axis to the right. The thermal ellipsoids are drawn at 50% probability level except for the hydrogen atoms which are drawn arbitrarily small for clarity.

are all consistent with a relatively weak interaction between Ni and TBC. The structure of tris(2,3-η^2-2,3-norbornene)nickel(0) in which the three alkenes are coplanar has been reported and the mean Ni–C bond length is 2.06 (3) Å.[15] These data along with the spectroscopic data (vide infra) indicate that although the nickel–alkyne interaction in Ni(TBC) is stronger than a nickel–alkene interaction, it may be weaker than typical nickel–alkyne interactions. A second in-plane complex of TBC, Cu(TBC)(OTf), has much less distortion of the alkynes.[31] A correlation between the C≡C—R angle and the C≡C bond length for 70 transition-metal π-bound alkyne complexes has appeared.[37] Compared to these complexes Ni(TBC) shows little distortion in the C≡C—R fragment.[38]

The ORTEP stereoview packing diagram viewed down the *c* axis (Figure 2) shows a slipped stack arrangement with the benzo groups eclipsed. A view down the *b* axis (Figure 3) shows a herringbone pattern with an interplanar distance of 3.35 (1) Å. The crystal structure of TBC shows the molecules are also slipped stacked[12] with an interplanar spacing of 3.29 Å and the benzo groups staggered. For comparison, slip stacking is also observed in the crystal structure of nickel phthalocyanine.[2e] The crystal packing may explain the air stability of crystalline Ni(TBC) as compared to reactivity of Ni(TBC) in solution as discussed below (vide infra). In the solid state the nickel atom is centered over the benzo group of the next Ni(TBC) molecule in the stack. This arrangement may prevent the approach of reactive species to the nickel atom.

Spectroscopic Characterization of Ni(TBC). The infrared spectrum of Ni(TBC) shows two bands at 1957 and 1983 cm^{-1} for the $\nu_{C\equiv C}$ stretch with a shoulder at 1963 cm^{-1} due to the ring modes of the benzo groups and is consistent with the distortion from D_{3h} symmetry as crystallographically determined. The IR spectrum of Ni(TBC) shows a relatively small shift of the $\nu_{C\equiv C}$ stretching band from that of the free ligand compared to other alkyne complexes of Ni(0).[10b,17,32,33] Complexes 1 and 2 have $\nu_{C\equiv C}$ bond stretches in the range 1810–1772 cm^{-1}. In complexes 1 and 2, the alkynes are considered four-electron donors and there is strong back-donation from the metal into the π^*-orbitals.[10a,16,36] The spectrum of Ni(TBC) is consistent with limited back-donation of nickel electron density into the π^*-orbitals of the alkynes, as is the structural data above.[39]

The ^{1}H NMR spectra of Ni(TBC) in benzene-d_6 and THF-d_8 show two multiplets in the AA′XX′ spin system.[23] The two types of protons are shifted downfield from the resonances in the free TBC molecule. The proton attached to C(13) (see Figure 1) is assigned to the downfield resonance because it is closer to the alkyne and is expected to be more deshielded. The spectra are solvent dependent with the shifts in THF-d_8 more downfield than those in benzene-d_6.[40]

Complete assignment of the ^{13}C NMR spectrum of Ni(TBC) was made by comparing its proton coupled ^{13}C NMR spectrum of the proton-coupled ^{13}C NMR spectrum of the free TBC and by obtaining the CP-MAS ^{13}C{^{1}H} NMR spectrum of Ni(TBC). The chemical shift of the alkyne carbons of TBC at 93.6 ppm is shifted downfield to 109.6 ppm in Ni(TBC). The 127.7 ppm resonances in TBC for the ipso-benzo carbons is shifted to 142.7 ppm in Ni(TBC). The sextet is assigned to C(14) (Figure 1). In addition to the proton on C(14), C(14) is coupled to the protons on C(13) and C(15). The ^{13}C NMR spectra for a number of Ni(0) π-alkyne complexes have been reported for the series $(Me_3P)_2Ni(\mu_2\text{-}RC{\equiv}CR)$ and (bis(dimethylphosphino)ethane)Ni(μ_2-RC≡CR) (R_1 = H, Me, Ph).[32] The range of chemical shifts in these complexes is 111.4–137.9 ppm for the alkyne carbons and 135.0–140.9 ppm for the ipso carbons when R is a phenyl group. The ^{13}C chemical shift for the alkyne carbons of $(\mu\text{-}C_6H_5C{\equiv}CC_6H_5)[Ni(COD)]_2$ has been reported to be 106.9 ppm.[29c]

The ^{13}C NMR chemical shifts for alkynes in d^{10} complexes tend to occur at lower field than in other transition-metal systems.[29,32] The change in shift in complexes of two-electron donor alkynes tends to be less than the change in shift in complexes of four-electron donor alkynes.[41] The geometry of Ni(TBC) is constrained such that

---

(37) Gervasio, G.; Rossetti, R.; Stanghellini, P. L. *Organometallics* **1985**, *4*, 1612–1619.

(38) Burns, C. J.; Andersen, R. A. *J. Am. Chem. Soc.* **1987**, *109*, 941–942.

(39) Nakamoto, K. *Infrared and Raman Spectra of Inorganic and Coordination Compounds*, 4th ed.; Wiley: New York, 1986; pp 386–391 and references cited therein.

(40) Barton, D. H. R.; Doering, W. *Applications of Nuclear Magnetic Resonance Spectroscopy in Organic Chemistry*: Pergamon: New York, 1969; 107–111.

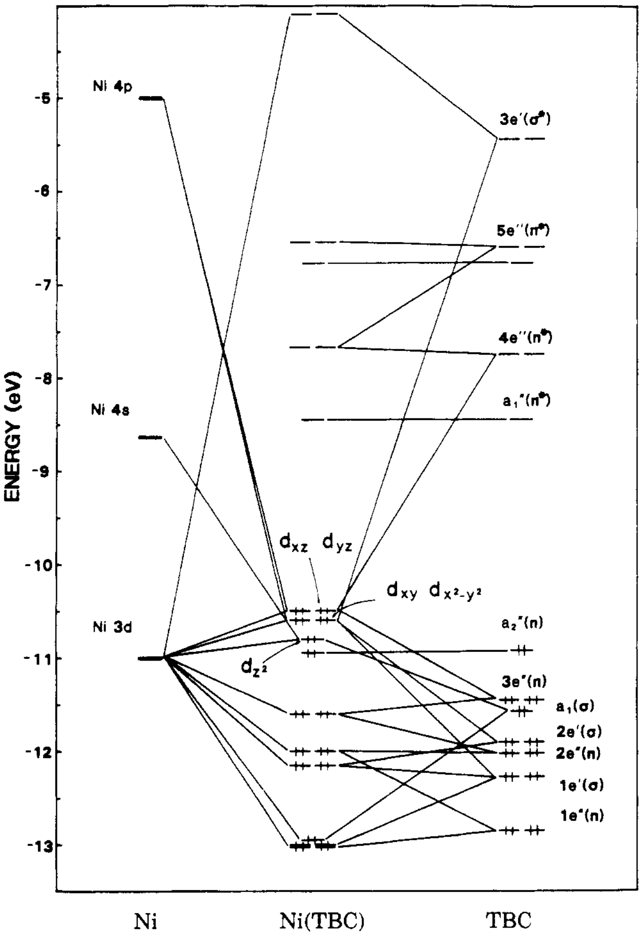

Figure 4. ASED-MO diagram for Ni(TBC).

the number of electrons donated by TBC is probably no more than 2e/alkyne. However, the small shift for $(\mu\text{-}C_6H_5C{\equiv}CC_6H_5)[Ni(COD)]_2$[18] (a classical four-electron donor alkyne complex) indicates that there are more factors determining the chemical shifts than the number of electrons donated by the alkyne.[42] The shift of the Ni(TBC) ipso-carbon resonance by 15 ppm downfield from the free ligand is nearly as large as the shift of the alkyne carbons, but this is not unusual for Ni(0) alkyne complexes.[32] The influence of the nickel center on these carbons appears to be strong. Also, the shift of the benzo ring protons downfield upon complexation of the nickel indicates that substitution on the benzo group can have a strong influence on the properties of the complex, consistent with the MO calculations.

The field desorption mass spectrum of Ni(TBC) shows a parent ion at 358.2 (5) amu. The calculated weight for $^{57}Ni(^{12}C_{24}{}^{1}H_{12})$ is 358.03 amu. The UV–vis spectrum shows a band at 587.5 nm (ϵ = 2.5 × 10^3, 2.11 eV) and a shoulder at 370 nm ($\epsilon \simeq 10^3$). The 587.5 nm band is assigned to a metal-to-ligand charge-transfer band. This is based upon its intensity and position as well as the results of the electrochemical experiments and MO calculations (vide infra). The spectrum of TBC is featureless to 340 nm.[3a] The spectroscopic and crystallographic characterizations are consistent with the three alkynes of the ligand each behaving as a two-electron donor to the metal making Ni(TBC) a 16-electron Ni(0) complex.

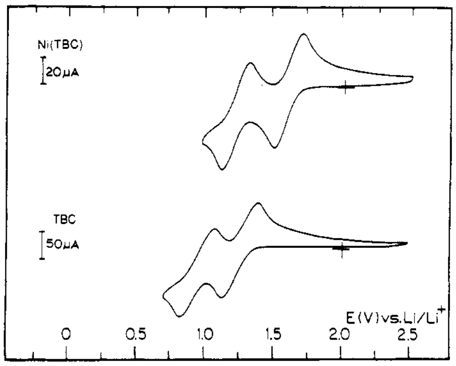

Figure 5. Typical cyclic voltammograms for TBC and Ni(TBC) at 100 mV s^{-1}.

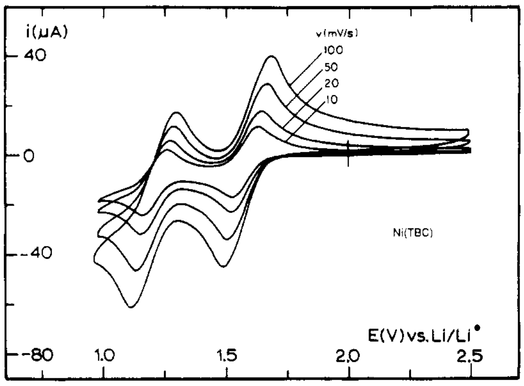

Figure 6. Variable scan rate (10–100 mV s^{-1}) cyclic voltammograms for Ni(TBC).

Table VI. Cyclic Voltammetry Results for TBC and Ni(TBC)

compd	$E_{p,a}(1)$	$E_{p,c}(1)$	$\Delta E_{p,a}(1)$	$E_{p,a}(2)$	$E_{p,c}(2)$	$\Delta E_p(2)$
TBC	1.39	1.13	0.26	0.98	0.73	0.25
Ni(TBC)	1.68	1.49	0.19	1.31	1.12	0.19

ASED-MO Calculations. The molecular orbital diagram for Ni(TBC) based on ASED-MO[28] calculations is shown in Figure 4. The results of the calculations indicate the HOMO is primarily metal centered with the LUMO primarily ligand centered. The LUMO of TBC drops a small amount in energy upon coordination of the nickel atom as determined in the cyclic voltammetry experiments. The two orbitals corresponding to the HOMO are the d_{xz} and d_{yz} orbitals.

Electrochemistry. Two reduction waves were observed for both Ni(TBC) and TBC. Cyclic voltammograms at 100 mV s^{-1} for TBC and Ni(TBC) in 0.1 M TBAP in THF are shown in Figure 5. The anodic ($E_{p,a}$) and the cathodic peak ($E_{p,c}$) potentials as well as the peak potential separations ($\Delta E_p = E_{p,a} - E_{p,c}$) are listed in Table VI. Figure 6 shows typical cyclic voltammograms for Ni(TBC) at different scan rates. The cathodic peak potentials shifted in a negative direction for each increase in the scan rate, and the peak potential separations were dependent of the scan rate, varying from 10 to 100 mV s^{-1}. However, the peak currents are proportional to the square root of the scan rate. These results suggest a moderately reversible redox process.[43] The electrochemical oxidation of Ni(TBC) led to an irreversible process at 3.5 V vs Li/LiBF$_4$. The cyclic voltammogram showed significant change upon cycling past this potential. This result is consistent with attempts to chemically oxidize Ni(TBC). The ASED-MO

---

[41] Templeton, J. L.; Ward, B. C. *J. Am. Chem. Soc.* **1980**, *102*, 3288–3290.

[42] (a) Karplus, M.; Pople, J. A. *J. Chem. Phys.* **1963**, *38*, 2803–2807. (b) Pople, J. A. *Mol. Phys.* **1963**, *7*, 301–306. (c) Salomon, R. G.; Kochi, J. K. *J. Organomet. Chem.* **1974**, *64*, 135–143.

[43] Bard, A. J.; Faulkner, L. R. *Electrochemical Methods, Fundamentals and Applications*; Wiley: New York, 1980; pp 213–246.

calculations show that the HOMO (vide supra) is a bonding orbital. Thus, removal of an electron results in destabilization of the complex. The reduction waves for Ni(TBC) are at a higher potential (reference to Li/LiBF$_4$) than the corresponding waves for TBC, indicating that the presence of a nickel atom in the TBC ligand results in lowering of the LUMO of TBC from the uncomplexed ligand.

A controlled potential electrolysis of Ni(TBC) was performed by maintaining the potential at 1.3 V vs Li/LiBF$_4$. This potential is between the first and second reduction waves (Figure 5). The solution slowly turned purple. Current was passed until 2 C were passed through 10 mL of a 5.2 × 10^{-4} M Ni(TBC) solution. The UV–vis spectrum showed a shift in the 587.5 nm band to approximately 600 nm with a concomitant increase in ϵ to $\sim 10^4$. The number of electrons passed per Ni(TBC) was approximately 1.

Reaction Chemistry. Solvent dependence of the rate of reaction of carbon monoxide with Ni(TBC) is observed. The relative rates of reaction for Ni(TBC) and CO in THF, C_6H_6, and Et$_2$O are 18:6:3. In contrast, with O$_2$ the relative rates of reaction in THF, C_6H_6, and Et$_2$O are 6:18:1. The solvent dependence is presumably due to the coordination strength of the solvent with Ni(TBC). The products of the reaction with C═O are Ni(CO)$_4$ and TBC, whereas the reaction with O$_2$ gives free TBC and an unidentified nickel compound. Ni(TBC) in benzene solution does not react with water. Crystals of Ni(TBC) are air-stable indefinitely while finely ground powders show release of TBC and the formation of paramagnetic materials in the presence of air (as evidenced by considerable broadening of the NMR resonances of the free TBC generated).

A range of reactivities is observed in the reactions of Ni(TBC) with the small molecules CDCl$_3$, CH$_3$CN, and CO$_2$. Decomposition of Ni(TBC) occurs in CDCl$_3$, but the TBC ligand remains intact. Interaction of CH$_3$CN or THF with Ni(TBC) results in a small downfield shift for ^{1}H NMR spectrum of Ni(TBC). However, these changes in the ^{1}H NMR spectra may be solvent effects. Ni(TBC) is unreactive toward CO$_2$ in benzene-d_6 solution.

Oxidation of Ni(TBC) with I$_2$ gives decomposition of the complex yielding TBC and probably NiI$_2$. These results are consistent with the electrochemical and theoretical results in that the oxidation is an irreversible process leading to decomposition. Conductivity is not observed because Ni(TBC), TBC, I$_2$, and NiI$_2$ are insulators.

Alkali-Metal Reduction of Ni(TBC) and TBC. Consideration of the decomposition associated with the oxidation of Ni(TBC), the cyclic voltammetry of Ni(TBC) and the reduction chemistry of transition-metal π-complexes[44] indicated that the reduction chemistry of Ni(TBC) should be explored. The initial experiments with lithium indicated that the reduction of Ni(TBC) to the dianion state was not complete. A material containing both Ni(TBC) monanion ($\nu_{C\equiv C}$ = 1873 cm^{-1}) and dianion ($\nu_{C\equiv C}$ = 1834 cm^{-1}) was obtained. The samples were quite unstable, especially toward dissolution without the aid of chelating agents for the alkali-metal cation. On the basis of IR data, reactions run in the presence of 18-crown-6, while showing improved results, either did not go to completion or showed decomposition. Several studies[45] have shown C222 (cryptand-(2.2.2)) to be a superior chelating agent for sodium and potassium compared to 18-crown-6. The use of C222 and sodium allowed the formation of solutions of mostly the monanion with some dianion of Ni(TBC). The reduction of Ni(TBC) by potassium in the presence of C222 proceeds smoothly with the color changing from deep blue (Ni(TBC)) to deep purple (Ni(TBC)$^-$) and then to red-brown (Ni(TBC)$^{2-}$). The formation of a purple monoanion is consistent with the constant potential electrolysis/UV–vis experiment described above. The dianion typically contains a trace of the monoanion.

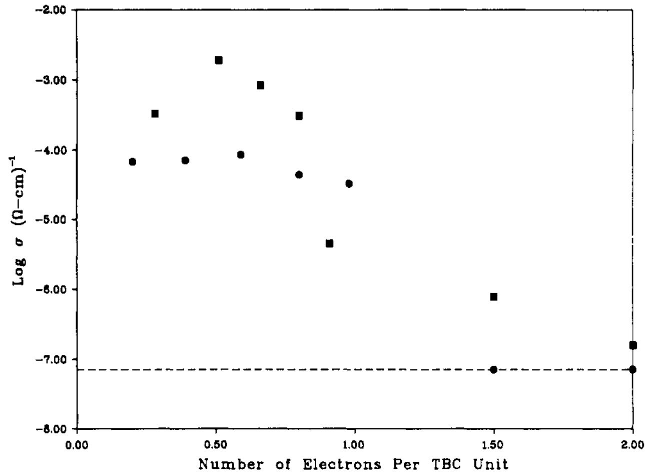

Figure 7. Conductivity versus number of electrons based upon initial stoichiometry for the doping study of Ni(TBC) with $[[K(C222)]_2][Ni(TBC)]$ (solid squares) and TBC with $[K(C222)]_x(TBC)$ ($x \simeq 2$)[25a] (solid circles). The dashed line represents the lower limit for conductivity measurements.

The IR spectrum of $[K(C222)]_2[Ni(TBC)]$ shows a sharp, relatively narrow band for $\nu_{C\equiv C}$ and a small shoulder for the monoanion contaminant. The ^{1}H NMR spectrum of the sample shows both free and complexed C222 as well as broadened THF peaks. The aromatic region of the ^{1}H NMR spectrum shows many complex peaks with multiplets similar in shape to that for Ni(TBC). These are postulated to be due to the presence of a diamagnetic singlet dianion. The presence of a small amount of the paramagnetic monoanion causes broadening of the spectrum of the diamagnetic dianion $[K(C222)]_2[Ni(TBC)]$. An EPR spectrum of the dianion shows only the presence of the monoanion impurity. The EPR spectrum of the monoanion (g_{iso} = 2.001, a_{iso} = 1.28 G, seven lines) is consistent with a planar delocalized monoanion[46] and is very similar to the spectrum of the monoanion of TBC previously reported.[3a] The hyperfine coupling seen in TBC$^-$ has not been observed in Ni(TBC)$^-$. The ^{1}H NMR spectrum of the species initially formed on reduction of Ni(TBC) with potassium and 18-crown-6 in THF-d_8 shows broad resonances in the 40–55 ppm region which are probably due to the paramagnetic monoanion.

To help clarify the mechanism of conduction of n-doped Ni(TBC) (vide infra), a parallel study on the reduction

---

(44) (a) Jonas, K.; Krüger, C. *Angew. Chem., Int. Ed. Engl.* **1980**, *19*, 520–537. (b) Jonas, K. *Adv. Organomet. Chem.* **1981**, *19*, 97–122. (c) Jonas, K.; Pörschke, K. R.; Krüger, C.; Tsay, Y. *Angew. Chem., Int. Ed. Engl.* **1976**, *15*, 621–622. (d) Jonas, K. *Angew. Chem., Int. Ed. Engl.* **1975**, *14*, 752–753. (e) del Rosario, R.; Stuhl, L. S. *Organometallics* **1986**, *5*, 1260–1262. (f) Pörschke, K. R.; Jonas, K.; Wilke, G.; Benn, R.; Mynott, R.; Goddard, R.; Krüger, C. *Chem. Ber.* **1985**, *118*, 275–297. (g) Wink, D. J.; Fox, J. R.; Cooper, N. J. *J. Am. Chem. Soc.* **1985**, *107*, 5012–5014. (h) Maher, J. M.; Fox, J. R.; Foxman, B. M.; Cooper, N. J. *J. Am. Chem. Soc.* **1984**, *106*, 2347–2353. (i) Collman, J. P.; Brothers, P. J.; McElwee-White, L.; Rose, E.; Wright, L. J. *J. Am. Chem. Soc.* **1985**, *107*, 4570–4571. (j) Collman, J. P.; McElwee-White, L.; Brothers, P. J.; Rose, E. *J. Am. Chem. Soc.* **1986**, *108*, 1332–1333. (k) Collman, J. P.; Brothers, P. J.; McElwee-White, L.; Rose, E. *J. Am. Chem. Soc.* **1985**, *107*, 6110–6111.

(45) (a) Pedersen, C. J.; Frensdorff, H. K. *Angew. Chem. Int. Ed. Engl.* **1972**, *11*, 16–25. (b) Boss, R. D.; Popov, A. I. *Inorg. Chem.* **1986**, *25*, 1747–1750. (c) Dietrich, B.; Lehn, J. M.; Sauvage, J. P. *Tetrahedron Lett.* **1969**, 2885–2888. (d) Akabori, S.; Ohtomi, M. *Bull. Chem. Soc. Jpn.* **1975**, *48*, 2991–2992.

(46) Drago, R. S. *Physical Methods in Chemistry*; W. B. Saunders: Philadelphia, 1977; pp 316–358, 436–466.

chemistry of TBC was performed. The IR spectrum of reduced TBC shows two bands at 2036 and 2089 cm^{-1} which have been assigned to the dianion and monoanion, respectively.

Doping of Ni(TBC) and TBC. The doping of Ni(TBC) with $Ni(TBC)^{2-}$ (or TBC with TBC^{2-}) resulted in a series of materials whose two-probe pressed powder conductivities are plotted in Figure 7. The results are promising because measurements by powder compaction methods typically yield values that are 10^2–10^3 smaller than the corresponding single-crystal values for anisotropic conductors[2e] and four-probe techniques yield values that can be 10^2–10^3 greater than the corresponding two-probe values.[47] Only a limited number of doping levels has been tested and the ideal doping level has not yet been determined. The peak conductivity occurs at approximately 0.5e/Ni(TBC). Each sample has been characterized by FT-IR. The intensity of the $\nu_{C\equiv C}$ band in Ni(TBC) decreases monotonically while the $Ni(TBC)^-$ $\nu_{C\equiv C}$ band increases with increasing proportion of $Ni(TBC)^{2-}$ dopant. The results of the TBC doping show a weak maximum at 0.6 e/TBC with a conductivity 25 times lower than the maximum observed for Ni(TBC). This indicates that while the presence of the nickel atom is not essential, it does have a strong influence on the conductivity. The maximum in the conductivity of doped Ni(TBC) (Figure 7) and the decreasing conductivity with more potassium shows that the conductivity is not the result of metallic impurities from potassium metal. Given the simlarities between TBC and phthalocyanine one might expect the mechanisms for conductivity to be similar in their transition metal complexes. Experimental work indicates $Ni(Pc)(I)_x$ conducts via the interacting π-orbitals of the macrocycle,[2e] while Co(Pc)(I) has been found to conduct via the metal spine.[2g] For n-doped Ni(TBC), current evidence supports conductivity through the π-orbitals of the macrocycle. The electrochemical results and theoretical calculations show the LUMO of Ni(TBC) is primarily ligand centered. In addition, nickel(0) is a d^{10} species requiring the 4s or 4p orbitals to be involved in order to form a conduction band for metal-centered conductivity. These orbitals are higher in energy and do not absorb the excess electron density when Ni(TBC) is reduced. Further studies on these compounds will include experiments to determine the mechanism of conductivity in n-doped Ni(TBC) and TBC.

The conductivity of doped Ni(TBC) is expected to be highly anisotropic.[1,2,48,49] Single crystals of the conducting materials have not been isolated thus far, but further attempts are being made to do so. Further work will include in depth studies on the reactivity of Ni(TBC) and its anions toward other small molecules, including carbon dioxide, and an examination of the chemistry of Ni(TBC) with other reducing agents, such as lithium naphthalenide. Further studies of doped Ni(TBC) and TBC will include magnetic susceptibility, EPR, and variable-temperature four-probe conductivity measurements.

Acknowledgment is made to the donors of the Petroleum Research Fund, administered by the American Chemical Society, and the Office of Naval Research for support of this work. Financial support for J.D.F. was provided by the BFGoodrich Fellowship at CWRU. We wish to thank Professor Daniel Scherson and Dr. Mark Daroux of the Case Center for Electrochemical Studies for helpful discussions and advice.

Registry No. TBC, 5385-26-2; C222, 23978-09-8; 18-crown-6, 17455-13-9; $Ni(COD)_2$, 1295-35-8; Ni(TBC), 98779-78-3; $[K(C222)]_2[Ni(TBC)]$, 121351-41-5; $Li_2[Ni(TBC)]$, 121351-42-6; Li[Ni(TBC)], 121372-69-8; [K(C222)]1$_2$(TBC), 121541-49-9; [K(C222)](TBC), 121351-44-8.

Supplementary Material Available: Tables of thermal parameters, calculated hydrogen positions, least-squares planes, and parameters for ASED calculations (2 pages); a listing of observed and calculated structure factors (8 pages). Ordering information is given on any current masthead page.

---

(47) (a) van der Pauw, L. J. *Philips Res. Rep.* **1958**, *13*, 1–9. (b) Valdes, L. B. *Proc. IRE* **1954**, 420–426. (c) Philips, T. E.; Anderson, J. R.; Schramm, C. J.; Hoffman, B. M. *Rev. Sci. Instrum.* **1979**, *50*, 263–265. (d) Coleman, L. B. *Rev. Sci. Instrum.* **1978**, *49*, 58–63.

(48) (a) Wudl, F. *Acc. Chem. Res.* **1984**, *17*, 227–232. (b) Maugh, T. H. *Science (Washington, DC)* **1983**, *222*, 606–607. (c) Williams, J. M.; Beno, M. A.; Wang, H.; Reed, P. E.; Azevedo, L. J.; Schirber, J. F. *Inorg. Chem.* **1984**, *23*, 1792–1793. (d) Greene, R. L.; Street, G. B. *Science (Washington, DC)* **1984**, *226*, 651–656. (e) Gamble, F. R.; DiSalvo, F. J.; Klemm, R. A.; Geballe, T. H. *Science (Washington, DC)* **1970**, *168*, 568–570. (f) Gressier, P.; Meerschaut, A.; Guemas L.; Rouxel, J.; Monceau, P. *J. Solid State Chem.* **1984**, *51*, 141–151.

(49) Etemad, S.; Heeger, A. J.; MacDiarmid, A. G. *Annu. Rev. Phys. Chem.* **1982**, *33*, 443–470.